



Double-layer focal plane microscopy for high throughput DNA sequencing

XIN ZHANG,^{1,*} KE KANG,¹ YANFANG JIANG,² JIAXUE HE,² AND YANFENG QIAO¹

¹*Changchun Institute of Optics, Fine Mechanics and Physics, Chinese Academy of Sciences, Changchun 130033, China*

²*Key Laboratory of Organ Regeneration & Transplantation of the Ministry of Education, Genetic Diagnosis Center, The First Hospital of Jilin University, Changchun, China*

*zhangxin@tju.edu.cn

Abstract: Throughput is one of the most important properties in DNA sequencing. We propose a novel double-layer focal plane microscopy that doubles the DNA sequencing throughput. Each fluorescence channel is divided into two tube lens channels by energy splitting, and the camera is adjusted to take images corresponding to different defocus positions of the objective, thus doubling the information capacity of the microscopy. The microscopy is applied to gene chip, which has high spatial frequency and good uniformity, so the simultaneous imaging of the two tubes has little influence on each other due to the spatial averaging effect. Experimental results show that the image signal to noise ratio (SNR) is reduced by 1%, while the sequencing throughput is doubled.

© 2022 Optica Publishing Group under the terms of the [Optica Open Access Publishing Agreement](#)

1. Introduction

High throughput DNA sequencing technology is one of the important methods in clinical and basic biomedicine [1–3]. The basic method of high-throughput DNA sequencing is massively parallel sequencing [4,5], among which fluorescence-based microscopy imaging is the most developed and widely used [6,7], and most commercial high-throughput sequencers are based on this method [8,9]. DNA molecules are broken into fragments containing hundreds of bases and loaded in submicron arrays onto a flat substrate to form a DNA sequencing chip. Fluorescent molecules label the first base of a DNA fragment, usually with two fluorescent coding correspondences or four fluorescence one-to-one correspondences, and the bases are then identified by fluorescence microscopy imaging. To generate sufficient fluorescence signal, each DNA fragment is amplified into hundreds of copies, forming hundred-nanometer scale spheres called DNA nanoball (DNB) [10,11], and each DNB can label hundreds of fluorescent molecules. After the first base is identified, the fluorescent molecule is removed by biochemical reaction, and then the second base is relabeled. Fluorescence imaging then identifies the second base, and this cycle is repeated hundreds of times to obtain the base sequence for each DNA segment. The entire DNA sequence can be obtained by data assembly. The size of DNA sequencing chip can reach more than 100 mm, and the DNB loaded on the chip can reach tens of billions. The biochemical process of the whole chip is carried out simultaneously, but the fluorescence microscopic imaging can only scan the entire chip one by one in small areas due to the limited optical information capacity, which is the bottleneck of the DNA sequencing throughput.

DNA sequencing throughput can be expressed as the product of optical information capacity and imaging speed, in which the imaging speed is limited by the camera, while the optical information capacity is limited by the numerical aperture and field of the objective, the core component of the microscopy [12]. The commonly used method to increase the information capacity is to directly increase the numerical aperture or view field of the microscopy [13,14]. This method relies on extremely complex optical-mechanical design, but due to the limitations of size,

weight, cost, and engineering difficulty, it is difficult to further improve sequencing throughput. The highest sequencing throughput achieved by this method is the released sequencing device DNBSEQ-T10×4RS [15], with a numerical aperture 1 and field of view of 2.1 mm and a single exposure resolution of 9 million DNBs. A single microscopy with a daily throughput of 50 whole genome sequencing, but weight nearly 2 tons and volume more than 1 cubic meter, limiting its application scenarios. Super resolution technique is an alternative method to improve information capacity without increasing numerical aperture and field of view [16–19]. Among super resolution technologies, structured light illumination is suitable for DNA sequencing and commercial products [20] have been released due to its simple composition, no special requirements for fluorescence labeling and wide field imaging. Super-resolution technology can improve information capacity because it can resolve more dense sample arrays, but the cost is that super-resolution images need to be obtained by rebuilding multiple exposure images, which is equivalent to exchanging spatial super-resolution for time consumption, so it is difficult to improve sequencing throughput.

In this paper, a double-layer focal plane microscopy for high-throughput DNA sequencing is proposed. By studying the changes of defocus conjugate aberrations and imaging characteristics of microscopy images, a method was proposed to increase optical throughput by adding a spatial dimension in the defocus direction, that is, multiple focal planes corresponding to their respective tube channels are simultaneously imaging. Although high throughput is achieved, it is only suitable for high spatial frequency specimen due to the interaction of imaging between multiple focal planes. The surface of DNA sequencing chip is a dense DNB array, which precisely meets the characteristics of high spatial frequency. Since DNB was attached to the substrate, we developed a practical prototype of a double-layer focal plane fluorescence microscopy for DNA sequencing verification. Compared with commercial sequencers, this prototype doubled the sequencing throughput with only an additional tube lens channel and simple adjustments.

2. Principle of double-layer plane microscopy

The main imaging optical pathway of modern microscopy is composed of objective and tube lens, both of which are infinite corrected optics. Specimen on the focal plane of the objective is imaged and magnified on the camera sensor, which is on the focal plane of the tube lens. Figure 1 shows the Gauss optics imaging optical pathway of the microscopy. O is the object on the focal plane of the objective, and I is the conjugate image on the focal plane of the tube lens. When the object deviates from the focal plane of the objective lens, its conjugate image also deviates from the focal plane of the tube lens in the same direction, as shown in plane O' and plane I', plane O'' and plane I''.

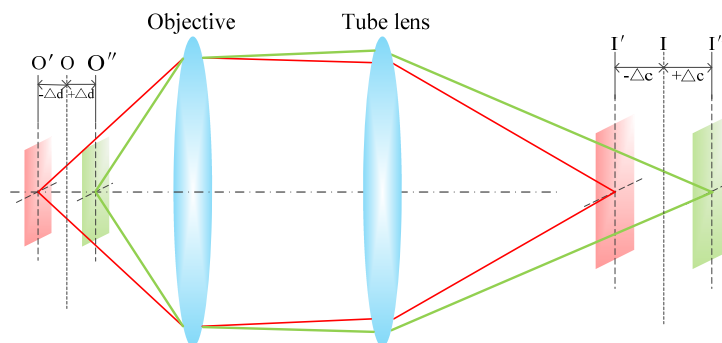


Fig. 1. Conjugate relation between objects and images in optical pathway of the microscopy.

In fact, there are aberrations in a real microscopy optical system consisting of multiple lenses. The infinity conjugate focal plane of the objective is the plane where the aberration correction is minimized, as is the tube lens. When the specimen deviates from the infinite conjugate focal plane, a relatively optimal imaging position can still be found, which is close to the Gaussian optical conjugate position, but the imaging quality is reduced due to the increase of aberration. The increment of geometric aberration depends on the optical design of the microscopy.

Figure 2 shows the increase in aberration caused by defocus imaging of a microscopy with a numerical aperture of 1 and magnification of 20, which was designed for our DNA sequencing prototype. The blue line in the figure is the position relation between the specimen and the relatively optimal image, which is approximately linear and close to the conjugate position of Gaussian optics. The black line in the figure is the corresponding wave aberration RMS, which increases approximately linearly in both directions away from the infinity conjugate focal plane. The sample deviates from the infinite conjugate focal plane within $\pm 6 \mu\text{m}$, the wave aberration RMS is less than 0.07λ , which meets the Marechal criterion [21], and the imaging quality is acceptable close to the diffraction limit. This range is far beyond the Depth of Focus (DOF), which is about $\pm 0.3 \mu\text{m}$. We define this range as Extensible Depth of Focus (EDOF).

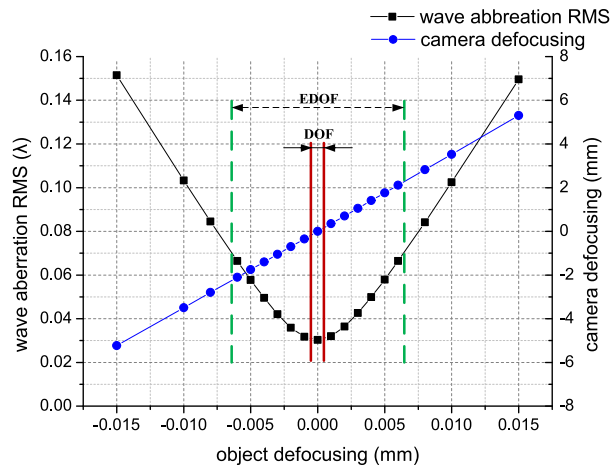


Fig. 2. The relationship between defocus imaging and aberration increase.

The above analysis indicates that the working distance of the microscopy can vary within EDOF, and the camera sensor is then adjusted to the corresponding conjugate position of the sample for high-quality imaging. In other words, the different defocus positions of the objective can simultaneously image high-quality in the multiple tube channels, which is equivalent to adding a dimension of light information throughput. Due to the energy splitting between multiple tube channels, which will reduce the signal intensity, and there is mutual crosstalk between channels, so the channels should not be too many. So, we propose a double-layer focal plane microscopy to improve the information throughput. The two focal planes are in a symmetric position with $\pm\Delta d$ before and after the infinity conjugate focal plane, so the two tube channels defocus $2\Delta d$ with each other, which results in uncompensated defocus aberration in both channels. Figure 3(a) shows the wave aberration RMS, which increases approximately linearly with defocus and has a maximum aberration of about 2λ at a EDOF defocus. Figure 3(b) ~ Fig. 3(i) show the simulated imaging of conjugate imaging and uncompensated defocus imaging on low spatial frequency specimen and high spatial frequency specimen respectively. The large aberration results in low spatial frequency specimen being blurred but their contour still exists, while high spatial frequency specimen become background with little fluctuation, that can be called the spatial averaging

effect. The simultaneous imaging of double-focal planes affects each other, which is equivalent to conjugate focused imaging superimposing defocused images. Superimposing blur contour on image is generally unacceptable, while superimposing background with little fluctuation is generally acceptable. Therefore, the double-layer focal plane microscopy does not require sophisticated optical design or complex defocus aberration correction system. However, the specimen is required to be high spatial frequency and uniform, which ensures the simultaneous imaging of the two tubes has little influence on each other. In addition, the upper sample of double-layer focal plane microscopy have occlusion effect on the lower sample. The blocking ratio of the upper sample should be small enough to ensure sufficient light flow for the lower sample. The Sequencing chips with a DNB diameter of 200-nm and array spacing of 500-nm have been used in the current commercial sequencers, such as MGI's DNBSEQ-T10×4RS sequencer. The double-layer chip can also be arranged according to this geometry pattern, and the blocking ratio is about 1/8, which is perfectly acceptable.

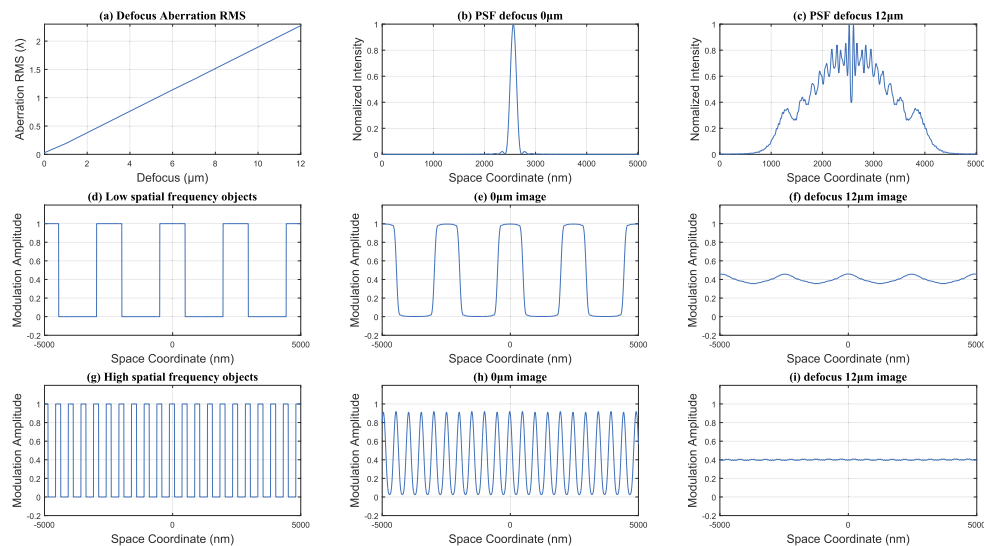


Fig. 3. Analysis of imaging characteristics of double-layer plane microscopy. (a) is the wave aberration RMS increasing approximately linearly with defocus. (b) and (c) are point spread function (PSF) at conjugate position and 12 μm defocus position. (d), (e) and (f) are low spatial frequency (400lp/mm) sample, conjugate image, and defocus image respectively. (g), (h) and (i) are high spatial frequency (2000lp/mm) sample, conjugate image, and defocus image respectively.

3. Imaging simulation of the DNA chip

Figure 4(a) shows the regular array of DNBs within a small region on the DNA chip surface, as seen under an atomic force microscopy (AFM). The randomness of the amplification process resulted in the difference of DNB size. The average size of DNBs is about 200 nm, the spacing is 500 nm, the corresponding spatial frequency is 2000 lp/mm, and the duty ratio is about 10%. Obviously, the DNA sequencing chip meets the specimen requirements of the double-layer focal plane microscopy proposed. Figure 4(b) shows the simulated image on the conjugate focal plane. The image is clear, and the DNBs can be distinguished. Figure 4(c) shows the simulated image at 1- μm defocus position, where the image becomes blurred, but the DNBs is faintly visible. Figure 4(d) shows the simulated image at 12- μm defocus position, in which no DNB can be distinguished in the image and only the background with little fluctuation is present. Defocused

images are equivalent to crosstalk between two channels in a double-focal plane microscopy. With the increase of defocus, the image approaches the uniform background, and the mutual influence becomes less. The above simulation shows that the DNA sequencing chip only needs very small defocus, then the two-channel imaging has little influence on each other. This guides us to build a double-layer focal plane microscopy for DNA sequencing.

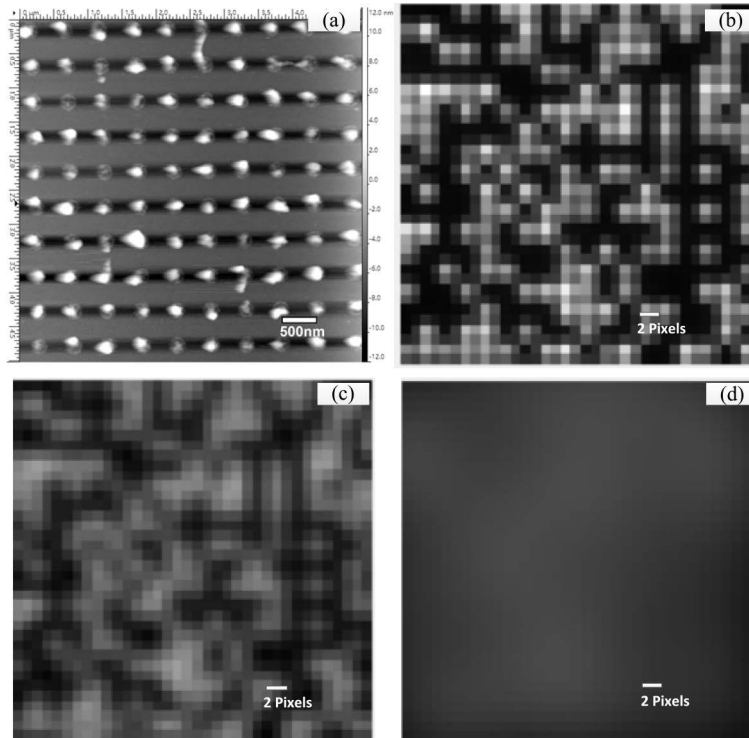


Fig. 4. DNA chip testing and imaging simulation. (a) AFM image of DNA chip. Each bright spot is a DNB with 500-nm spacing. (b) The simulated focused image of DNA chip. The magnification ratio between pixel and DNB is 2, that is, the object is 500 nm and the projection on the image is 2 pixels. (c) The simulated image of DNA chip defocused at 1 μm position. (d) The simulated image of DNA chip defocused at 12- μm position.

4. Imaging result with double-layer focal plane microscopy prototype

Based on the above analysis and simulation, we designed a double-layer focal plane microscopy for high-throughput DNA sequencing. Two fluorescence channels were set up in the microscopy to identify four bases by fluorescence binary coding. The optical layout is shown in Fig. 5(a), and the corresponding prototype is shown in Fig. 5(b).

The real image characteristics of DNA sequencing chip in focus and defocus position was tested by the prototype. The chip is first placed in the focal plane of one of the channels for imaging. Then control the loading platform to move the chip to different defocus positions for imaging. Figure 6(a) shows an image of a local small region of the chip in the focal plane, where DNB is easy to distinguish. In the upper left corner of Fig. 6(a) is the gray histogram, which spans a wide gray scale because it contains more detailed information. We extracted the information through background subtraction, Gaussian fitting, and subpixel interpolation, then a new intensity histogram was generated as shown in Fig. 6(b), in which the area with larger gray scale is DNB information whose average intensity is 20.1, and the area with smaller gray scale

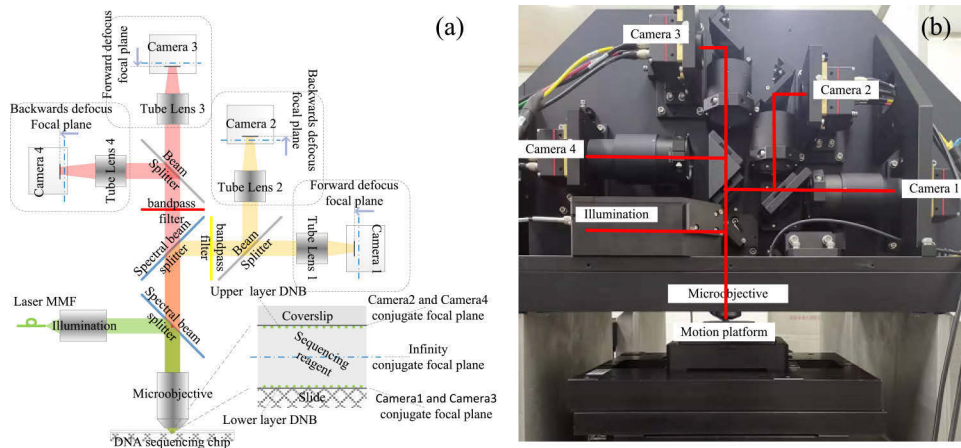


Fig. 5. (a) layout of the double-layer focal plane microscopy for DNA sequencing. DNA sequencing chip is flow-cell structure, and DNB is distributed on the reagent immersion surface of the silicon slide and the glass coverslip to form a double-layer chip. As the excitation light, the laser is delivered from the multi-mode fiber. The excitation light is homogenized by the integrating rod in the illumination system, and then projected onto the infinity conjugate focal plane of the objective in the way of critical illumination. The upper and lower sample planes have appropriate defocus of several micrometer, which can not only ensure sufficient illumination uniformity, but also eliminate the effect of the tiny defects on the end face of the rod due to blurring of the spots. Emission fluorescence is divided into two spectral channels by a spectral beam splitter. Then each channel is split into two paths by an energy beam splitter. In each of those two paths the fluorescence is focused on the camera by a tube lens. There are two cameras in each fluorescence channel, camera 1 and 2 in one channel, while camera 3 and 4 in the other channel. Cameras 1 and 3 are forward-defocused, conjugated to the lower layer focal plane of the microscopy. Cameras 2 and 4 are backward-defocused, conjugated to the upper layer focal plane of the microscopy. (b) Prototype of the double-layer focal plane microscopy for DNA sequencing. The prototype was modified from a four-channel fluorescence microscopy. The secondary spectral beam splitter is replaced by an energy beam splitter. The cameras are defocused as described in the layout.

is background whose average intensity is 0 after background subtraction. The mean difference between the signal and the background is the average signal, and the background is approximately normally distributed, so the standard deviation (STD) of the background is noise which is 1.86. The average SNR is then obtained, which is 10.8 at the focal plane position. Figure 6(c) and Fig. 6(d) show defocused images of $1\mu\text{m}$ and $6\mu\text{m}$, respectively. As expected, the larger the defocus, the more blurred the image. The $1\mu\text{m}$ defocus image still shows blurred DNB, while the DNB of the $6\mu\text{m}$ image has completely disappeared, leaving only the background with little fluctuation. The upper left corner of Fig. 6(c) and Fig. 6(d) is the gray histogram of defocused image, which is approximately normal distribution. With the increase of defocus, the STD of gray distribution becomes small, and the image approaches the uniform background.

In double-layer chip imaging, the imaging of each channel is equivalent to the superposition of focused image and defocused image. To determine the reasonable spacing between the two focal planes for this DNA sequencing prototype, the chip was imaged with spacing of $1\mu\text{m}$ within EDOF. Then STD of the gray histogram varies with the defocus distance was obtained, as shown in Fig. 8. The SNR of the superimposed images of each defocused image and the focused image is also calculated, as shown in Fig. 7. From the curves, for defocusing distances of about $6\mu\text{m}$ or

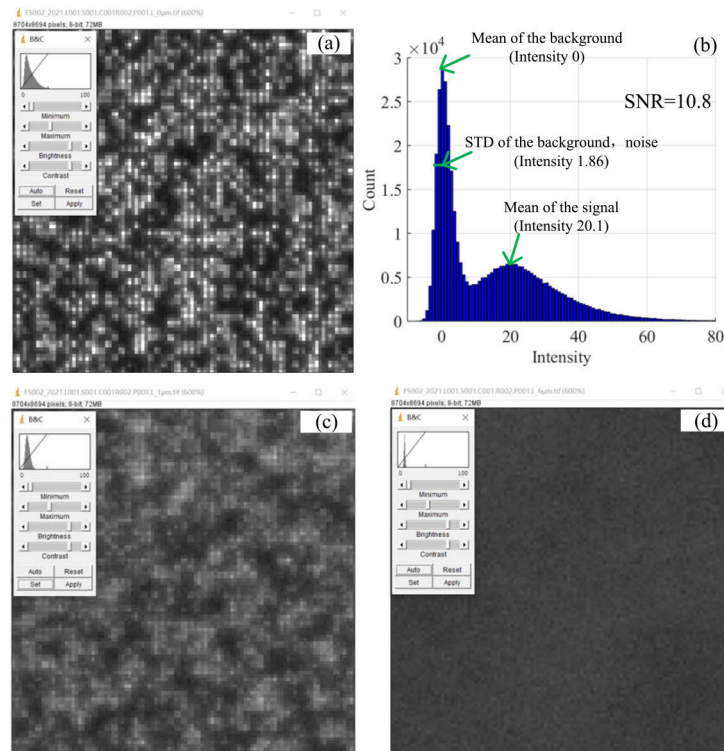


Fig. 6. Imaging test of DNA sequencing chip. (a) Focused image. The gray histogram is shown in the upper left corner. (b) Extracted intensity histogram. (c) and (d) The images of DNA chip defocused at 1µm and 6µm position respectively. The gray histograms are shown in the upper left corner.

more, the STD curve gets flatter and is close to the noise level of the camera itself, and the SNR curve also gets flatter and is close to the level of the focused image. Therefore, the spacing of the two-layer focal plane between 6 -12 µm is suitable for this prototype, which can reduce the crosstalk between the two channels and ensure good imaging quality.

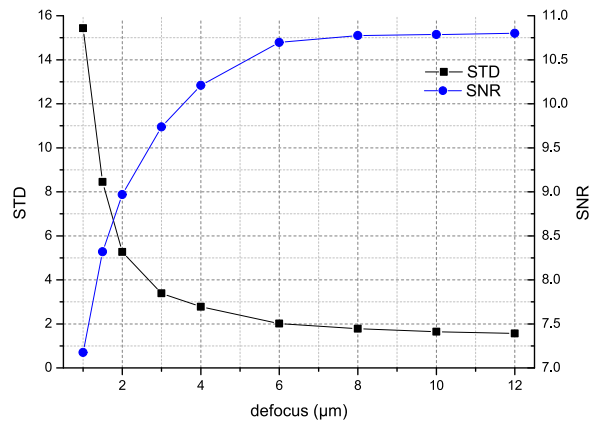


Fig. 7. The relationship between double chip spacing and image quality.

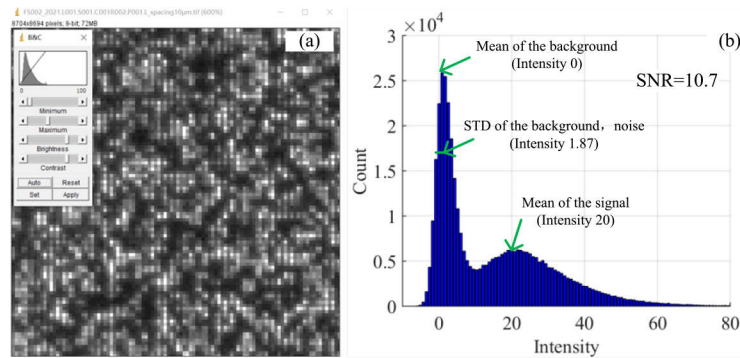


Fig. 8. Imaging test and SNR of double-layer chips gapped $10\mu\text{m}$ on the prototype. The gray histogram is shown in the upper left corner of Fig. 8(a). (b) Extracted intensity histogram.

Double-layer chips gapped $10\mu\text{m}$ apart was used to validate the double layer focal plane microscopy. The cameras of the two channels are respectively adjusted to the conjugate position corresponding $\pm 5\text{-}\mu\text{m}$ defocusing from the infinity conjugate focal plane of the objective. Figure 8(a) shows a small area of the image of camera 1. In the upper left corner of Fig. 8(a) is the gray histogram, which spans a wide gray scale because it contains more detailed information. Figure 8(b) shows the intensity histogram obtained after processing, with SNR of 10.7. By comparing Fig. 8(a) to Fig. 6(a), the image sharpness is similar. By comparing Fig. 8(b) and Fig. 6(b), the SNR decreases by about 1%. The reason is that the crosstalk signal received by camera A is not a uniform background, resulting in increased noise. Although 1% SNR loss reduces a little sequencing quality, the benefits of doubling the throughput and halving the cost are well worth it.

5. Conclusion

This paper presents a double-layer focal plane simultaneous imaging method for DNA sequencing. Due to the high spatial frequency and uniform characteristics of DNA sequencing chip, double-layer DNB with different defocus positions corresponds to different tube channels simultaneously imaging with little influence on each other, which is equivalent to doubling the information capacity of the optical system, providing an alternative technical route for improving sequencing throughput. The prototype has been built and high-quality imaging has been obtained. Future work will focus on the development of the sequencing equipment with real-time focusing scanning imaging of double-layer chip.

Funding. Bethune Center for Medical Engineering and Instrumentation (BQEGCZX2019032).

Acknowledgement. The authors are thankful to Yizhu Zhang for useful discussions.

Disclosures. The authors declare that there are no conflicts of interest related to this article.

Data availability. Data underlying the results presented in this paper are not publicly available at this time but may be obtained from the authors upon reasonable request.

References

1. M. C. Wendl and R. K. Wilson, "Aspects of coverage in medical DNA sequencing," *BMC Bioinformatics* **9**(1), 239 (2008).
2. J. M. Rizzo and M. J. Buck, "Key Principles and Clinical Applications of "Next-Generation" DNA Sequencing," *Cancer Prev. Res.* **5**(7), 887–900 (2012).
3. S. Goodwin, J. D. McPherson, and W. R. McCombie, "Coming of age: ten years of next-generation sequencing technologies," *Nat. Rev. Genet.* **17**(6), 333–351 (2016).
4. Y. H. Rogers and J. C. Venter, "Genomics: massively parallel sequencing," *Nature* **437**(7057), 326–327 (2005).
5. G. Gao and D. L. Smith, "Clinical Massively Parallel sequencing," *Clinical Chemistry* **66**(1), 77–88 (2020).

6. L. Gao and Z. Lu, "The removal of fluorescence in sequencing-by-synthesis," *Biochem. Biophys. Res. Commun.* **387**(3), 421–424 (2009).
7. X. Zhang, F. Zeng, Y. Li, and Y. Qiao, "Improvement in focusing accuracy of DNA sequencing microscopy with multi-position laser differential confocal autofocus method," *Opt. Express* **26**(2), 897–906 (2018).
8. NovaSeq™ 6000, Illumina, Inc., <https://www.illumina.com/systems/sequencing-platforms/novaseq.html>.
9. Genetic Sequencer DNBSEQ™-T7, MGI Tech Co., Ltd., https://en.mgi-tech.com/products/instruments_info/5.
10. Q. Li, X. Zhao, W. Zhang, L. Wang, J. Wang, D. Xu, Z. Mei, Q. Liu, S. Du, Z. Li, X. Liang, X. Wang, H. Wei, P. Liu, J. Zou, H. Shen, A. Chen, S. Drmanac, J. S. Liu, L. Li, H. Jiang, Y. Zhang, J. Wang, H. Yang, X. Xu, R. Drmanac, and Y. Jiang, "Reliable multiplex sequencing with rare index mis-assignment on DNB-based NGS platform," *BMC Genomics* **20**(1), 215 (2019).
11. Y. Chen, H. Wang, J. Yang, H. Yang, W. Zhang, R. Drmanac, and C. Xu, "Reusable and sensitive exonuclease III activity detection on DNB nanoarrays based on cPAS sequencing technology," *Enzyme Microb. Technol.* **150**, 109878 (2021).
12. I. J. Cox and C. J. R. Sheppard, "Information capacity and resolution in an optical system" J," *J. Opt. Soc. Am. A* **3**(8), 1152–1158 (1986).
13. C. A. Werley, C. M. Ping, and A. E. Cohen, "Ultrawidefield microscopy for high-speed fluorescence imaging and targeted optogenetic stimulation," *Opt. Lett.* **8**(12), 5794–5813 (2017).
14. Y. Zhang and H. Gross, "Systematic design of microscopy objectives. Part I: System review and analysis," *Adv. Opt. Techn.* **8**, 313–347 (2019).
15. Total Solutions for Population Genomics, <https://en.mgi-tech.com/products/solution/7>.
16. S. W. Hell and J. Wichmann, "Breaking the diffraction resolution limit by stimulated emission: stimulated-emission-depletion fluorescence microscopy," *Opt. Lett.* **19**(11), 780–782 (1994).
17. E. Betzig, G. H. Patterson, R. Sougrat, O. W. Lindwasser, S. Olenych, J. S. Bonifacino, M. W. Davidson, J. L. Schwartz, and H. F. Hess, "Imaging intracellular fluorescent proteins at nanometer resolution," *Science* **313**(5793), 1642–1645 (2006).
18. M. J. Rust, M. Bates, and X. Zhuang, "Sub-diffraction-limit imaging by stochastic optical reconstruction microscopy (STORM)," *Nat. Methods* **3**(10), 793–796 (2006).
19. H. Zhang, X. Chen, T. Zhu, C. Yi, and P. Fei, "Adaptive super-resolution enabled on-chip contact microscopy " Opt," *Opt. Express* **29**(20), 31754–31766 (2021).
20. NextSeq™ 1000 and NextSeq 2000, Illumina, Inc., <https://www.illumina.com/systems/sequencing-platforms/nextseq-1000-2000.html>.
21. E. Born and Wolf, *Principles of Optics*, 7th ed. (Cambridge University, UK, 2002).